Electroporation characteristics of human primary T cells

Pinar Aksoy*, Bulent Arman Aksoy*, Eric Czech*, Jeff Hammerbacher*
* Microbiology and Immunology Department at Medical University of South Carolina

Abstract

Electroporation is the most feasible material delivery system for genetic manipulation of human primary T cells. These T cells are notoriously harder to transfect in their unstimulated state compared to the activated ones; however, the reasons behind this phenomenon are poorly characterized. Here, we show that both electroporation and transfection efficiency of a T cell highly depends on its cellular state, where T cells with central memory (CM) phenotype are more likely to die upon electroporation but also are easier to transfect compared to the other T cell phenotypes—namely naive and effector memory (EM). Our data suggests that material delivered into T cells is less likely to localize into the nucleus in a non-dividing cellular state compared to a dividing one. Moreover, the CM phenotype within an unstimulated pan T cell population has different transfection and proliferation properties than the CM population that recently emerged from the naive population upon activation. These different electroporation, transfection, and proliferation characteristics across different T cell phenotypes can have important practical implications, such as genetic engineering of T cells for adoptive cell transfer (ACT) therapy.

Introduction

Adoptive T cell therapy (ACT) has proven to be an effective therapeutic strategy for some cancer types, such as lymphoma, and it has been shown to generate promising rates of complete or partial responses for a majority of patients. T cells used for ACT can be obtained in different ways, *e.g.* tumor infiltrating lymphocyte cultures or genetically engineered T cells isolated from the periphery, depending on the target tumor type (Restifo, Dudley, and Rosenberg 2012).

The common workflow for adoptive cell transfer based immunotherapy involves isolation of lymphocytes from patient's blood and then activation of the pan T cells to make them amenable to engineering. There is evidence from previous and ongoing clinical trials that particular T cell subtypes or culturing techniques can directly affect the efficacy of ACT and the therapy outcome. For example, clinical response to ACT has been shown to correlate with the fraction of

particular T cell subsets used for ACT, where less differentiated, or more stem-like, T cells now correlate with a better clinical response (Klebanoff, Gattinoni, and Restifo 2012). Similarly, profiling peripheral T cell clones from ACT patients allowed others to nominate new biomarkers (*e.g.* TET2 promoter disruption) for more effective T cell populations (Fraietta et al. 2018). However, activation of pan T cells, which is required for *ex vivo* expansion and genetic manipulation, results in a decrease in the naive subset. With the studies suggesting that "younger cells do better at immunotherapy", the field has started focusing on the end population that is going to be infused back to the patients to make it more naive-like before infusion (Restifo, Dudley, and Rosenberg 2012) (Hinrichs et al. 2008).

Although viral and non-viral delivery systems are commonly used in activated T cells for genetic manipulation within the clinical or research setting, the reasons why unstimulated T cells are hard to transduce or transfect have not been extensively studied. Here, we characterize different T cell populations with regards to their electroporation and transfection efficiencies to better understand why efficiencies vary highly across these cells. We identify potential barriers to successful transfection of particular T cell subtypes with a plasmid DNA and discuss practical considerations for efficient genetic manipulation of unstimulated T cells.

Results

Activated T cells can more efficiently be transfected compared to unstimulated T cells

Unstimulated T cells isolated from peripheral blood mononuclear cells (PBMCs) of healthy donors and their anti-CD3/CD28 bead activated counterparts were electroporated with a GFP plasmid on the second day of activation. The transfection efficiencies were measured the following day by flow cytometer. Unstimulated cells had considerably lower transfection efficiencies compared to their activated counterparts 4.1% and 49.46%, respectively (Figure 1).

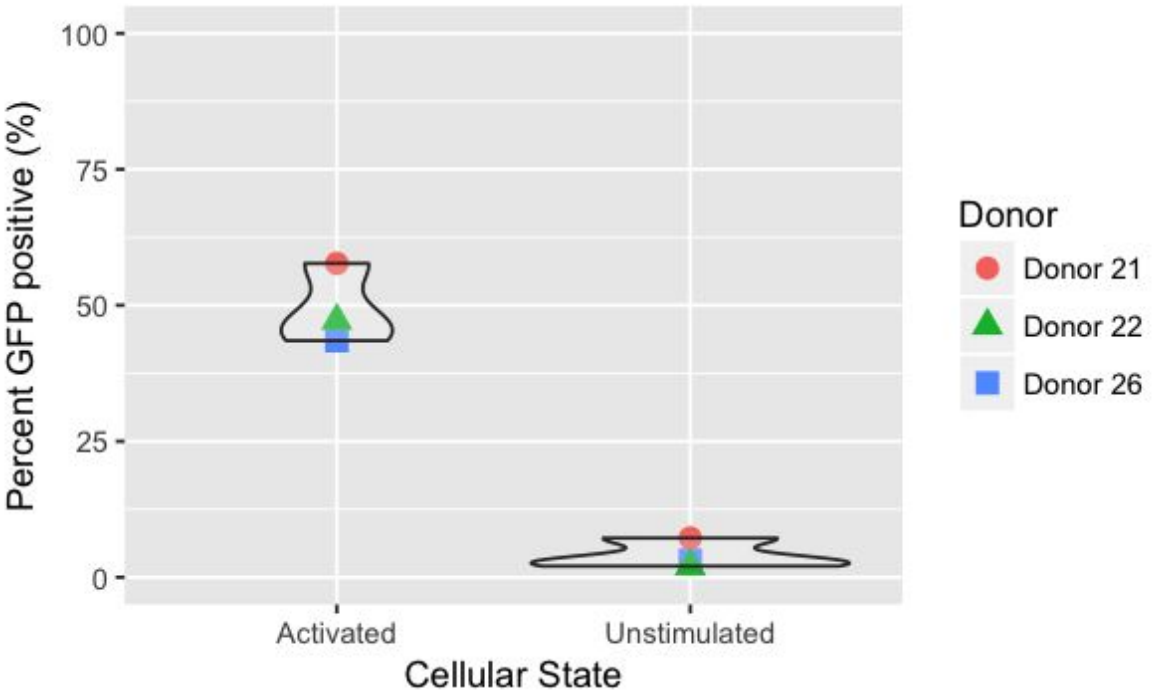

Figure 1. Unstimulated T cells have very low transfection efficiencies compared to activated T cells. Unstimulated and CD3/CD28 bead activated T cells were electroporated on the second day of activation with a GFP plasmid (7.5 ug DNA per 1 million cells) using Neon electroporation device. The next day, GFP expression was analyzed by flow cytometer. See this notebook for detailed data and analysis.

Unstimulated pan T cells can be electroporated with a plasmid at comparable levels to activated cells

Given the very low transfection efficiencies of the unstimulated T cells, we wanted to know if they were able to take up nucleic acids via electroporation on a level comparable to activated T cells. For that, we covalently labeled an empty pCMV6 plasmid with a fluorophore (Cy5) using a nucleic acid labeling kit and electroporated the unstimulated and activated cells on the second day of activation with the labeled plasmid. We incubated the cells for 15 minutes in the cell culture incubator and then collected half of the cells for analysis by flow cytometer right away. The rest of the cells were analyzed by flow cytometer the next day of electroporation. Repeating the experiment with 3 donors, we detected more than 60% plasmid positive cells for unstimulated group and more than 90% for activated group when the cells were collected 15 minutes after electroporation (Figure 2). The next day, the frequency of plasmid positive cells declined for both groups but it was still more than 40% for unstimulated and almost 80% for activated groups (Figure 2).

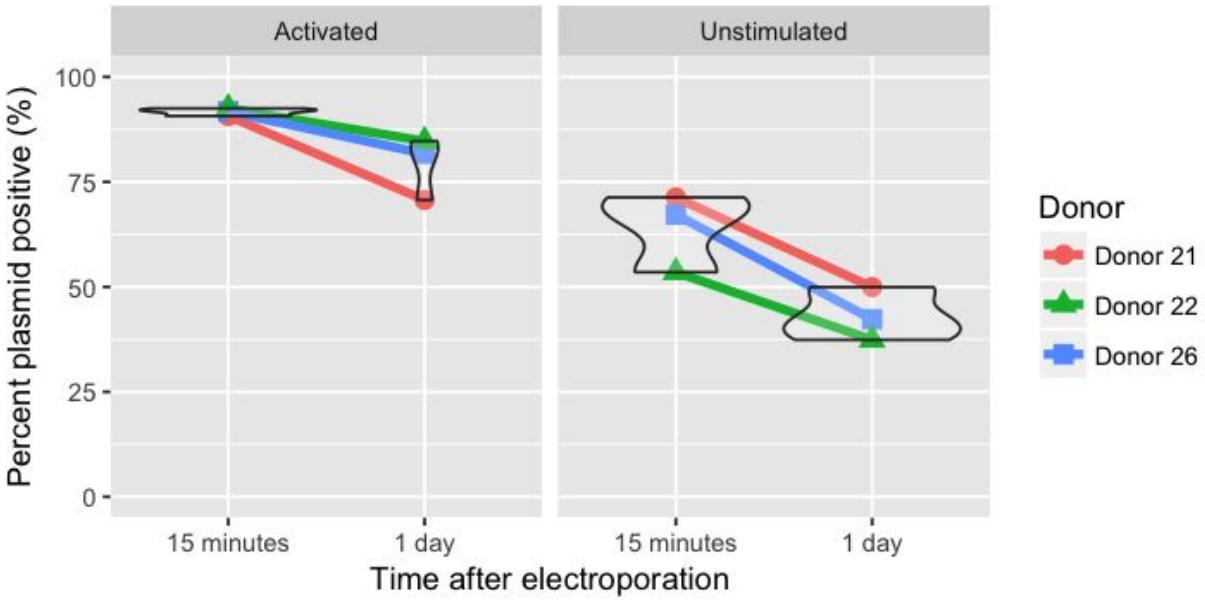

Figure 2. Electroporation of labeled plasmid DNA into activated and unstimulated T cells. Anti-CD3/CD28 bead activated or unstimulated cells were electroporated with a Cy5-labeled empty pCMV6 plasmid. The cells were cultured for 15 minutes and for 1 day and the percentage of labeled plasmid positive cells were analyzed by flow cytometer. See this notebook for detailed data and analysis.

Intracellular localization of the plasmid DNA is different across activated and unstimulated T cells

The above results suggested that the electroporation efficiency of activated and unstimulated cells were comparable, whereas the transfection efficiency of each group was considerably different than each other. For a successful transfection event, the electroporated plasmids should localize to the cell nucleus for gene expression. Based on the difference in transfection and electroporation efficiency of unstimulated cells, we hypothesized that within the activated group the frequency of plasmids that were in the nucleus would be higher than the unstimulated group. For this, we electroporated each group with the Cy5-labeled-pCMV6 (empty plasmid) and fixed the cells on microscope slides the following day. We also ran aliquots of the same samples on flow cytometer to double check the frequency of plasmid positive cells in each group. The fixed cells were stained with DAPI to visualize the cell nuclei and phalloidin to stain the actin cytoskeleton to estimate the cell borders. The plasmid was visualized by its fluorophore-conjugate. The cells were scanned under a fluorescence microscope and the frequency of plasmids that were localized to the nucleus was estimated by Cytokit (Figure 3b, Supplemental Table 1**)** (Czech et al. 2018). Briefly, the plasmid assumed to be in the nuclei if 90% of the plasmid signal overlaps with the DAPI signal. Based on our results with 4 donors, the frequency of cells with nuclear plasmids was higher in activated cells with a level of almost 60% for the activated cells and 20% for the unstimulated cells (Figure 3a).

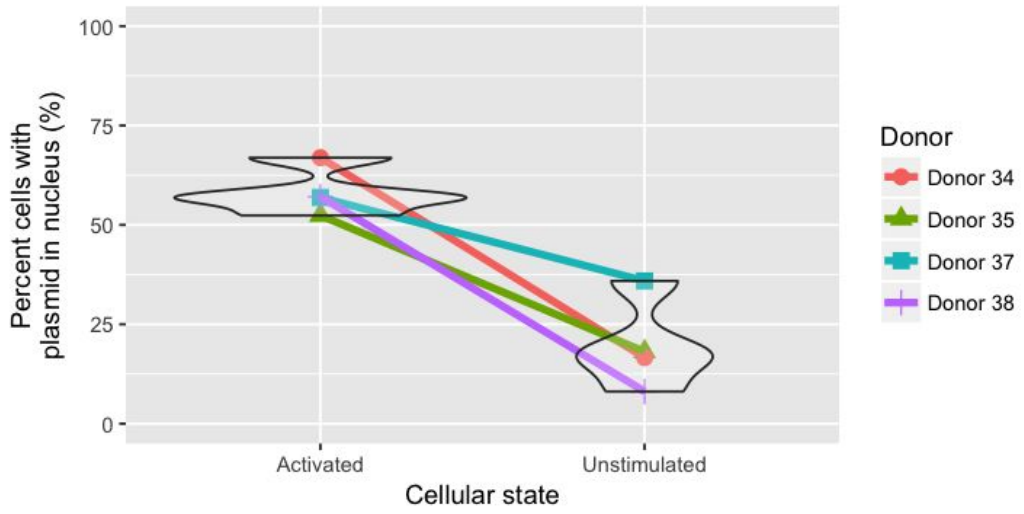
100
75
50
25
0
Percent cells with plasmid in nucleus (%)
Activated
Unstimulated
Cellular state
Donor
Donor 34
Donor 35
Donor 37
Donor 38

(a)

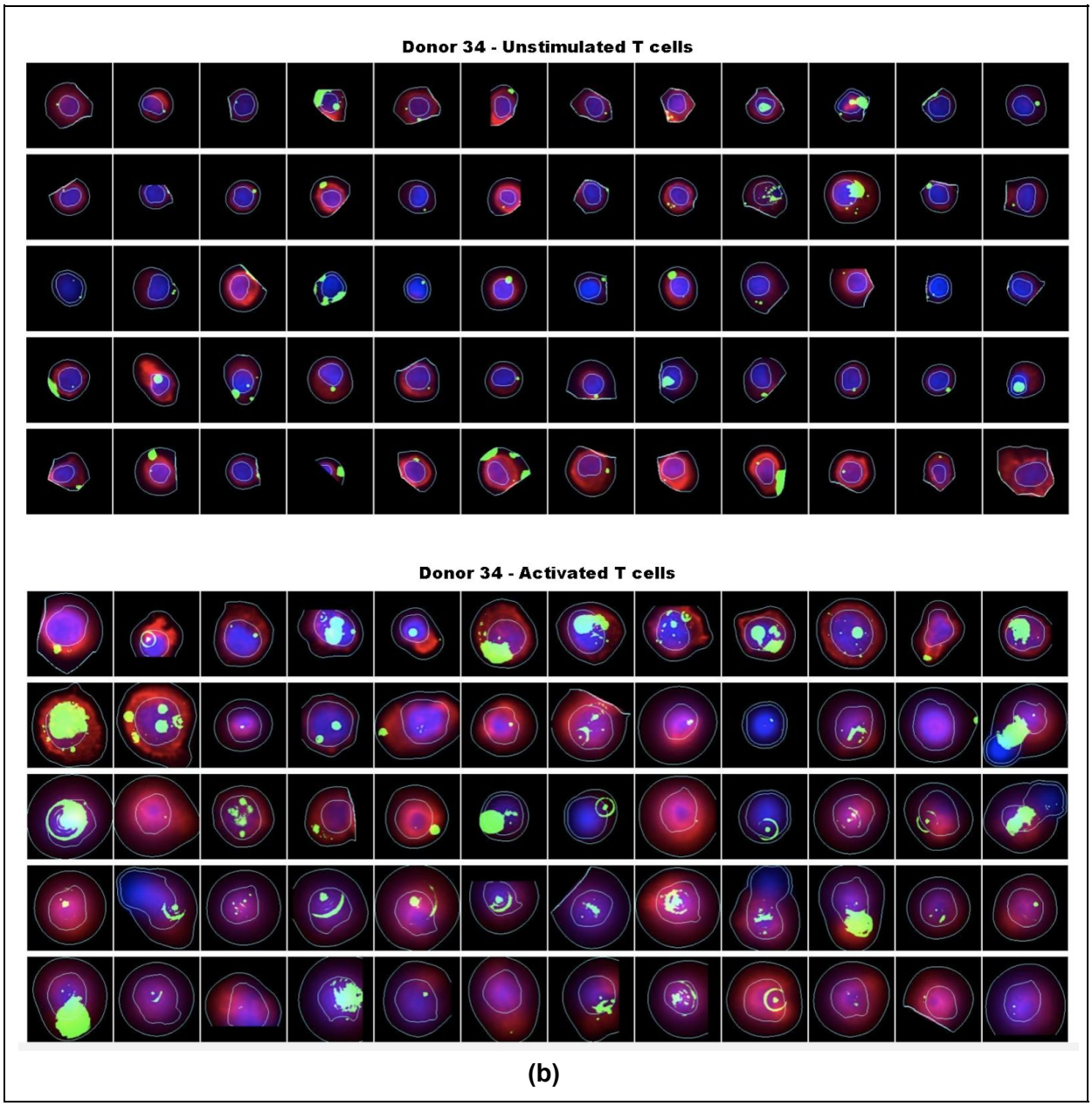

Figure 3. Imaging of the labeled plasmid electroporated cells 24 hours after electroporation. Cy5-labeled-pCMV6 was electroporated into unstimulated and anti-CD3/CD28 bead activated cells on the second day of activation. The cells were incubated for a day and then they were fixed on slides. (a) The frequency of cells with nuclear plasmid was higher in activated T cells compared to unstimulated T cells. See this notebook for detailed data and analysis. (b) Cytokit was used to analyze the microscope images (Czech et al. 2018). Each sub-panel shows 60 representative individual cells that were plasmid positive. Cell, nucleus, and plasmid signal borders as well as the signal intensities are shown as inferred via Cytokit's detection algorithm (Red: phalloidin, green: Cy5-labeled-plasmid, blue: DAPI). See Supplemental Table 1 for detailed inferred cellular characteristics.

Activating the cells post-electroporation does not increase transfection efficiencies of unstimulated T cells

Because our microscope results suggested that the plasmid DNA remained mostly cytoplasmic in unstimulated cells, we tried activating these cells immediately after electroporation to facilitate nuclear localization of the intracellular plasmid. Studies showed that the commitment for cell cycle entry occurs 3-5 hours post activation and the first cell division is completed around 30-48 hours post activation (Lea et al. 2003; Chapman and Chi 2018). Our flow results showed that the plasmid DNA remained within almost half of the unstimulated cells a day after electroporation (Figure 2). Therefore, we hypothesized that the transfection efficiency might increase when the cells were activated immediately after electroporation because the plasmid should still be in the cytoplasm when the nuclear envelope breaks down as the cells start proliferating upon activation. To test this, we first electroporated the unstimulated cells with a GFP plasmid and then immediately activated the cells for 2 days with anti-CD3/CD28 beads or phorbol 12-myristate-13-acetate (PMA)/ionomycin. After 2 days of activation, the frequency of GFP positive cells were analyzed by flow cytometer. The results with four donors showed that none of the activation methods significantly increased the transfection efficiency (Figure 4).

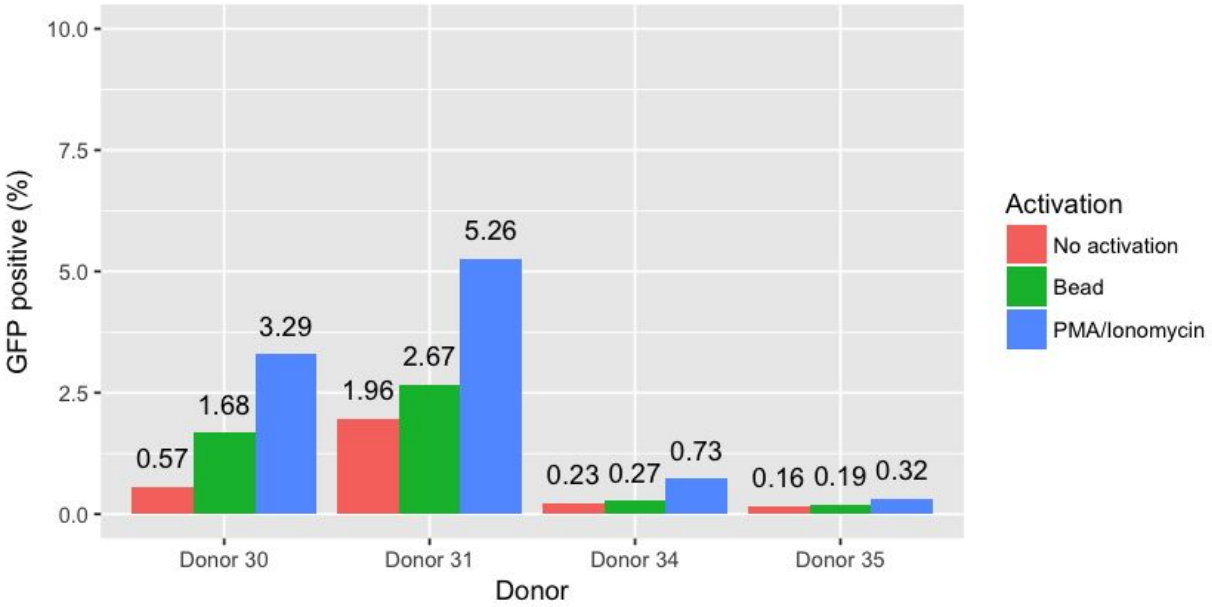

Figure 4. Activation of the cells after electroporation does not increase transfection efficiencies of unstimulated cells. Unstimulated cells were electroporated with a GFP plasmid and the cells were immediately plated in cell culture media with anti-CD3/CD28 beads or PMA/ionomycin. The cells in the “no activation” group was plated in regular T cell culture media. The GFP expression was analyzed 2 days after electroporation. See this notebook for detailed data and analysis.

Different T cell subgroups have different electroporation and transfection efficiencies

These results made us hypothesize that not all subpopulations within an unstimulated pan T cell population are electroporated and transfected with a similar efficiency. If, for example, the electroporation and transfection efficiency of naive cells are the lowest among the others to start with, then even activating these cells following electroporation cannot increase the transfection efficiency. To compare the electroporation efficiency of each subpopulation, we electroporated unstimulated T cells from 3 donors with a Cy5 labeled pCMV6 plasmid and analyzed the frequency of plasmid positive cells 15 minutes after electroporation. To estimate the frequencies of each subpopulation, we stained the cells with CD45RO and CCR7 antibodies. For both CM (CD45RO+ CCR7+) and EM (CD45RO+ CCR7-) groups, plasmid positive cell frequency was higher than the plasmid negative cell frequency. However, naive cells (CD45RO- CCR7+) were mostly plasmid negative (Figure 5).

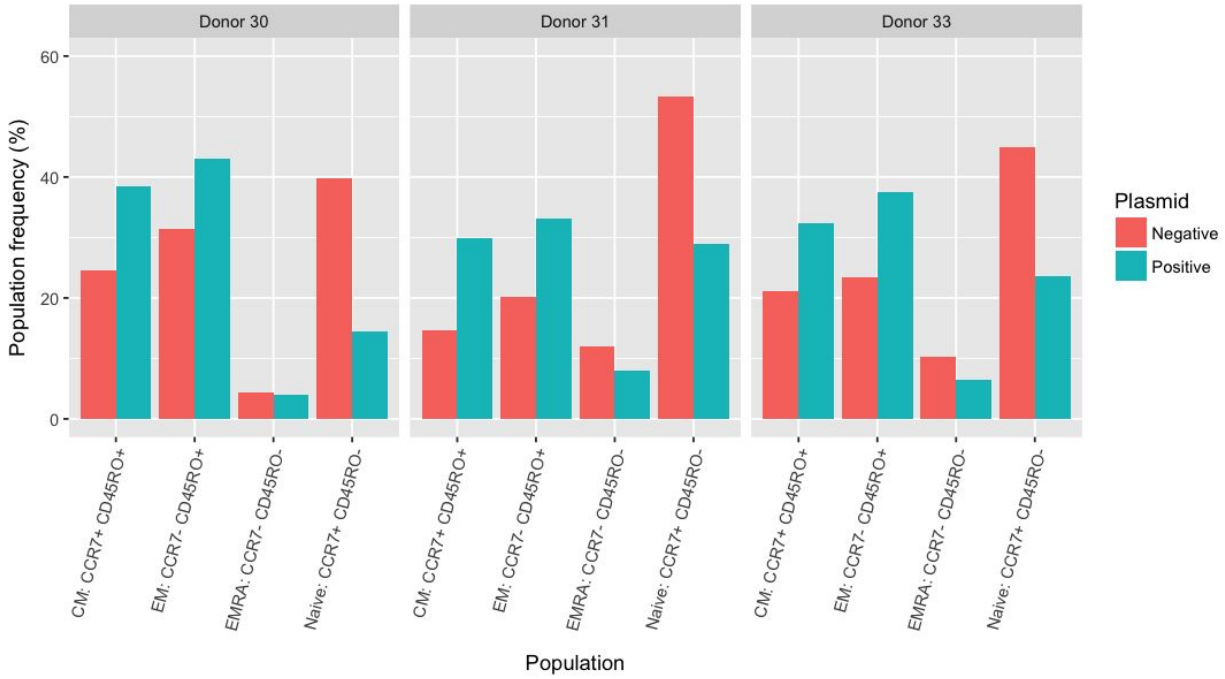

Figure 5. Electroporation efficiencies of unstimulated pan T cell subsets. Unstimulated T cells were electroporated with Cy5-labeled-pCMV6 and the frequency of cells with the labeled plasmid was analyzed 15 minutes after incubation with the plasmid. Memory cells were mostly labeled-plasmid positive, whereas naive cells were mostly negative. See this notebook for detailed data and analysis.

Then, we also compared the transfection efficiency of the subpopulations within unstimulated and activated groups using 3 donors and a GFP plasmid. Activation was performed with

anti-CD3/CD28 beads and the cells were activated for 2 days. On the second day of activation, the cells were debeaded and electroporated. The next day, the frequency of GFP positive cells within each subpopulation were analyzed by flow cytometer. For both activated and unstimulated groups, the CM subpopulation was the only one with more GFP positive cells than GFP negative ones (Figure 6). Given that the proliferative capacity of the CM subpopulation is the highest among the others, it is not surprising to see the same trend for the transfection efficiency as well (Reiser and Banerjee 2016)

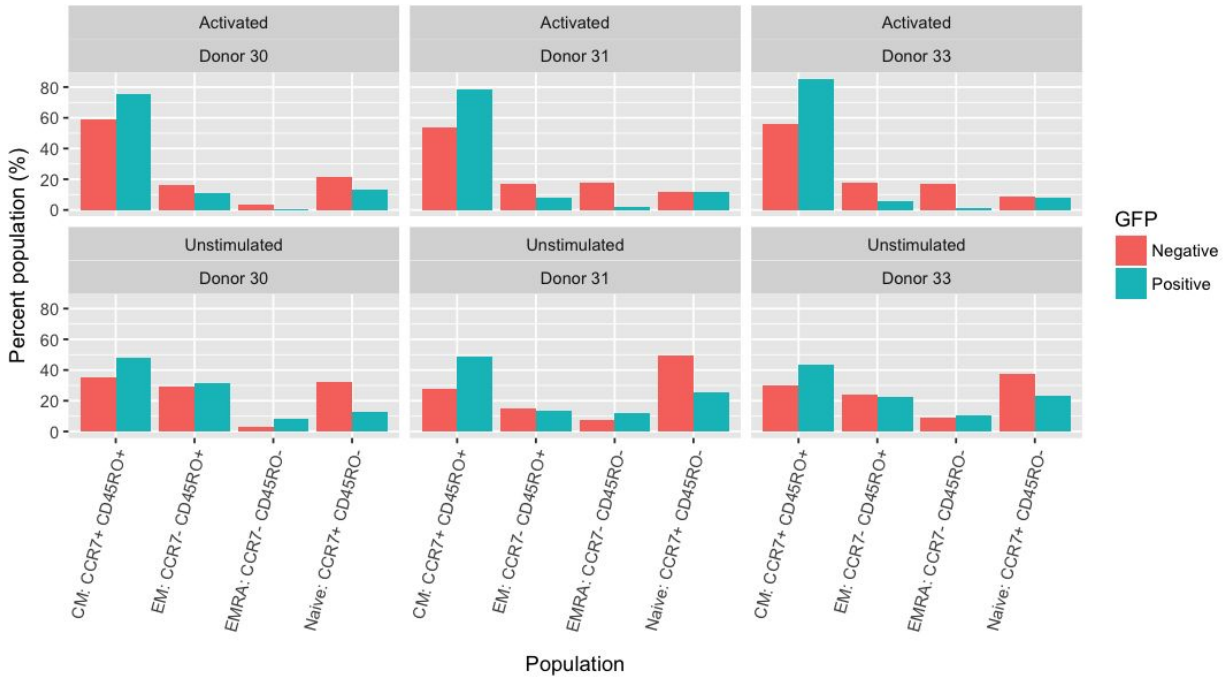

Figure 6. Transfection efficiencies of pan T cell subsets. Unstimulated and anti-CD3/CD28 bead activated T cells were electroporated on the second day of activation with a GFP plasmid. The GFP expression of each subset was analyzed 24 hours electroporation. CM subset has the highest transfection efficiency within both unstimulated and activated pan T cells. See [this notebook] for detailed data and analysis.

Viability of each T cell subgroup can vary upon plasmid DNA electroporation

Next, we analyzed the cell viability of each subpopulation within an unstimulated group from 2 donors upon mock electroporation and electroporation with a GFP plasmid. The frequencies of each subpopulation were analyzed using CD45RO and CD45RA antibodies and we estimated cell death by comparing the cell frequencies of experimental groups to the no electroporation group. On the same day of electroporation, when the cells were analyzed only 15 minutes after electroporation, we did not observe any difference in the population frequencies of any subgroups compared to no electroporation condition. However, when the cells were incubated

for a day and analyzed the next day, we found that for EM and CM groups DNA electroporation was more detrimental than the empty electroporation (Figure 7). These results suggested that the CM subpopulation has the highest transfection efficiency among the others, however it was also more vulnerable to electroporation with a DNA plasmid compared to others.

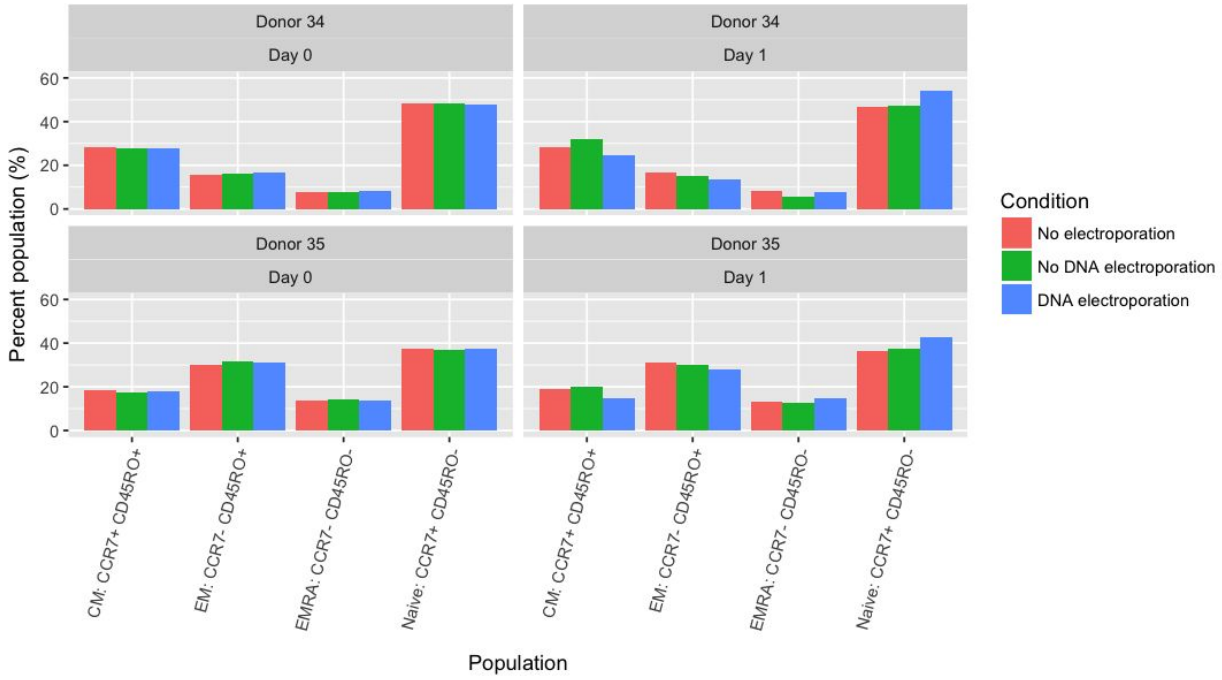

Figure 7. Viability of unstimulated pan T cell subsets upon electroporation. Unstimulated T cells from 2 donors were either electroporated with empty plasmid or with electroporation buffer only. The control group was not electroporated and the cells were directly seeded into the recovery plate. The cell subset frequencies analyzed 15 minutes and 24 hours after electroporation by flow cytometer. Compared to the mock electroporation, CM cells died the most upon DNA electroporation. See [this notebook]() for detailed data and analysis.

Profile of an activated T cell population differs based on the profiles of the starting unstimulated population

Activating the unstimulated cells immediately after electroporation did not significantly increase the transfection efficiencies, which was surprising given that these cells still had the plasmid one day following electroporation (Figures 2 and 3b). We decided to enrich the pan T cell population for naive (CD45RO-) or memory phenotypes (CD45RA-) to better characterize the proliferation capacities of each subgroup. CD45RO depletion via antibody-based negative selection gave us almost a pure population of naive cells together with a small EMRA group and CD45RA depletion gave us almost a pure population of memory cells (Supplemental Figure 1). The cells

were activated for 2 days with anti-CD3/CD28 beads, debeaded, and the subpopulation frequencies were analyzed at day 2 and day 5 of activation.

Upon activation for 2 days, for the CD45RO depleted group (mostly naive), almost 70% of the naive population became CMs and the rest remained as naive cells, suggesting that activation with anti-CD3/CD28 beads was not 100% effective (Figure 8). We did not detect any enrichment for the EMs when naive cells were activated with the antibody coated beads. When activated for 2 days, CD45RA depleted group (CMs and EMs) showed an increase in the CM frequencies and a decline in the EM frequencies. Cell counts were also decreased for activated EMs in the CD45RA depleted group for all 3 donors, however cell counts increased for 2 out of 3 donors for the activated CMs. Similar to the CD45RO depleted group, no-depletion group's cell frequencies were also in favor of CMs. The successfully activated naive cells increased the frequencies of the CMs within pan T cell population and not all of the naive cells were activated.

On the 5th day of activation within the CD45RO depleted group, naive population frequency decreased due to actively proliferating CM population. For the CD45RA depleted group, the frequencies of CMs and EMs did not change; CM frequency was higher and EM frequency was lower when these cells were activated. Interestingly, we observed that the proliferative capacity of newly activated CMs was better (1.45 ∓ 0.75 fold, n=3) than the CMs that were isolated from the PBMCs.

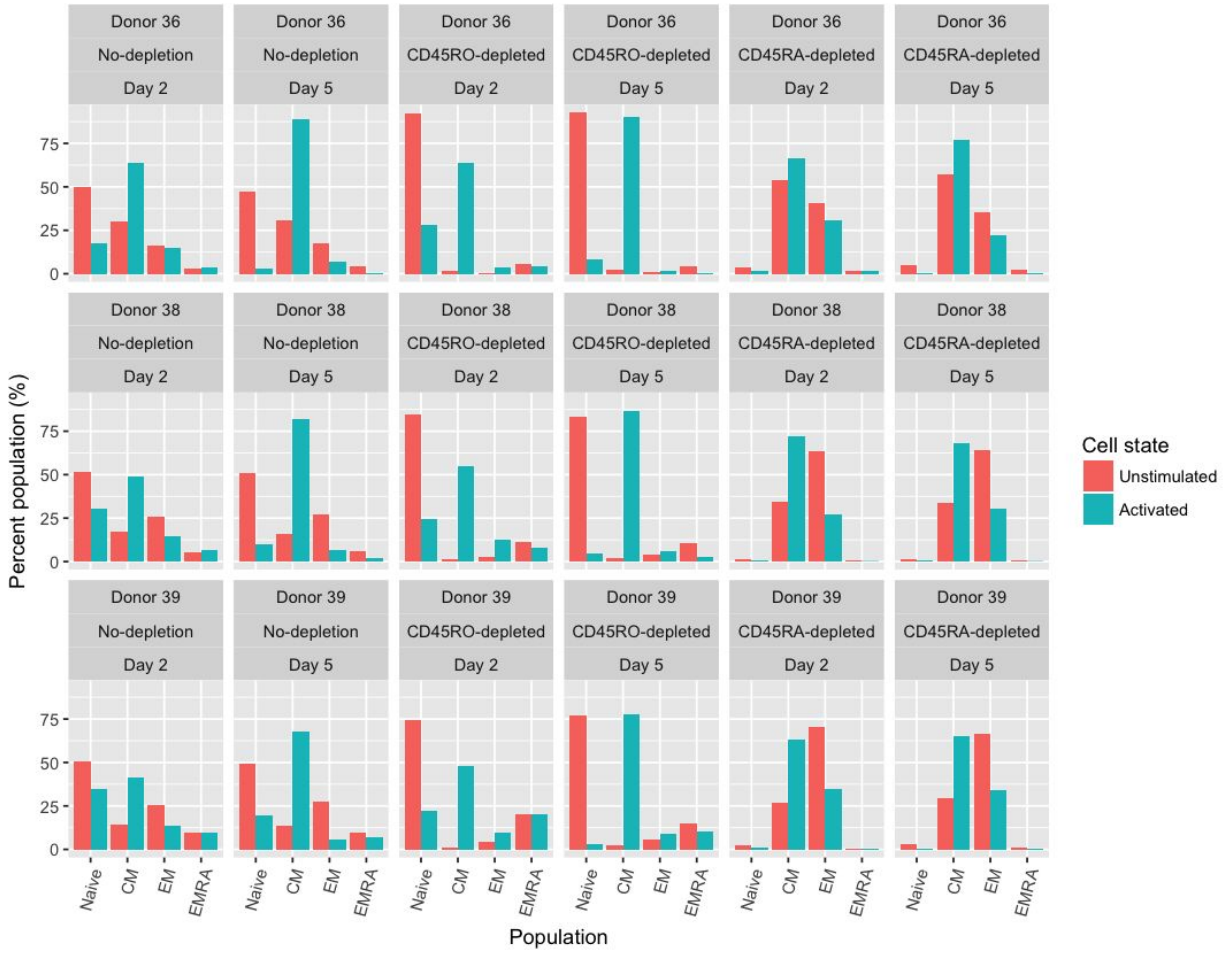

Figure 8. Profiling of naive and memory subsets upon activation. Naive and EMRA cells were enriched via CD45RO depletion and CM and EM cells were enriched via CD45RA depletion. Upon depletion with corresponding antibodies, each group was activated via CD3/CD28 beads for 2 days. On the second day of activation, the cells were debeaded and analyzed for subset frequencies. Some of the cells were cultured for 3 more days for analyzing on the 5th day of activation. No depletion group was included as a baseline control. See this notebook for detailed data and analysis.

Materials and Methods

Human primary T cell culture

PBMCs were isolated from healthy human donors by Ficoll centrifugation (Lymphocyte separation medium, Corning). T cells were isolated using Dynabeads Untouched Human T Cells Kit using manufacturer's protocols (Thermo Fisher). Isolated T cells were kept in T cell media: RPMI with L-glutamine (Corning), 10% fetal bovine serum (Atlas Biologicals), 50 uM 2-mercaptoethanol (EMD Millipore), 25 mM HEPES (HyClone), 1% Penicillin-Streptomycin (Thermo Fisher), 1X sodium pyruvate (HyClone), and 1X non-essential amino acids (HyClone)

All of the cells were supplemented with 200 IU/ml of IL-2 (National Cancer Institute). T cells were activated for 2 days with anti-CD3/CD28 magnetic dynabeads (Thermo Fisher) at a beads to cells concentration of 1:1, with supplement of IL-2.

Protocol details:

- Culture media: DOI:10.17504/protocols.io.qu5dwy6
- PBMC isolation from buffy coat: DOI:10.17504/protocols.io.qu2dwye

Plasmids

- pcDNA3.3_NDG was a gift from Derrick Rossi (Addgene plasmid # 26820).
- pcDNA3.3_eGFP was a gift from Derrick Rossi (Addgene plasmid # 26822).
- pCMV6-Entry Tagged Cloning Vector was purchased from OriGene (#PS100001).

Electroporation of T cells

After 2 days of activation, the cells were collected and put in a centrifuge tube. The tube was placed on DynaMag (Thermo Fisher) and the magnetic beads were removed. Activated and unstimulated cells were centrifuged for 7 minutes at 300 x g, the supernatant was aspirated and the cell pellet was resuspended in T buffer (Thermo Fisher). When working with Neon 10 ul tip, 200,000 cells were resuspended in 9 ul of T buffer and 1.5 ug DNA was added. Electroporation was performed at 1600 V 10 ms 3 pulses settings using Neon electroporation device (Thermo Fisher). Upon electroporation, the cells were seeded on the recovery plate with T cell media and 200 IU/ml of IL-2. For a 24-well-plate, 5 reactions were seeded per well (a total of 1 million cells) with 0.5 ml T cell media.
For the imaging experiment, 3 Neon-100 ul reactions (6 million cells and 45 ug labeled DNA in total) were electroporated and plated on a 12-well-plate with 3 ml T cell media.
For the electroporation experiment, where we activated the cells immediately after electroporation, we included anti-CD3/CD28 beads or PMA/ionomycin (Biolegend) in the recovery plate. Once the cells were electroporated, they were immediately cultured in activation media.

Plasmid labeling with Label-IT kit

100 ug of pCMV6 plasmid was labeled with 55 ul of Cy5 Label-IT kit for 1 hour at 37°C (Mirus Bio). The labeled plasmid was purified by ethanol precipitation. In brief, 0.1 volume of 5M sodium chloride and 2.5 volumes of ice cold 100% ethanol was added to the reaction. The solution was mixed and the tube was kept at -20°C for at least 30 minutes. Following the centrifugation and ethanol wash, the DNA pellet was resuspended in 10 mM Tris-Cl buffer (pH 8.5) and the DNA absorbance was read at A260 by NanoDrop One (Thermo Fisher) to quantify the eluted DNA.

Staining and imaging of T cells

The cells were collected and centrifuged at 300 x g for 5 minutes. The supernatant was discarded and the cells were washed once with PBS. Then, the cells were resuspended in PBS and 16% formaldehyde (Thermo Fisher #28908) was added at a final concentration of 4%. The cells were fixed for 30 minutes at 4°C. After incubation, the cells were pelleted and washed twice with 1X BD Perm/Wash buffer (BD Biosciences #554714). After the washes, the cells were stained with Alexa Fluor 488 Phalloidin (Thermo Fisher #A12379) for 30 minutes at room temperature in dark. After the incubation, the cells were pelleted and washed with PBS. In the end, the cells were resuspended in PBS and cytospinned on microscope slides by centrifugation for 5 minutes at 500 x g. After the spin, 1 drop of ProLong Glass Antifade Mountant with NucBlue Stain (Thermo Fisher #P36983) was added on the slide and the cells were covered with a coverslip. The cells were visualized by Keyence BZ-X710 fluorescence microscope at 60X.

Protocol details: DOI:10.17504/protocols.io.vede3a6.

Image analysis with Cytokit

Image analysis was conducted using Cytokit pipelines configured to segment nuclei over U-Net probability maps (McQuin et al. 2018) followed by secondary (cell boundary) and tertiary (plasmid body) object detection using threshold images resulting from Phalloidin and labeled plasmid channels. All image objects were subjected to morphological and minimum intensity filters before establish nucleus localization frequencies for plasmid objects, and parameters for this filtering were varied in a sensitivity analysis to ensure that findings are robust to processing configuration. Single cell image visualizations were generated using Cytokit Explorer. Raw imaging data sets are publicly available at the following Google Storage URL: `gs://cytokit/datasets/dna-stain`.

Antibodies

Name	Vendor	Catalog #
CD45RO	Biolegend	304210
CCR7	Biolegend	353212
CD45RO (depletion)	Biolegend	304202
CD45RA (depletion)	Biolegend	304102

Depletion by CD45RO and CD45RA antibodies

To deplete different subsets of cells within a pan T cell population, we used Dynabeads Pan-Mouse IgG (Thermo Fisher #11041) and followed the manufacturer's protocol for the negative isolation and indirect technique. The depleted cells were activated as described above with the anti-CD3/CD28 beads or kept as unstimulated cells.

Flow Cytometry

Flow cytometric analysis was performed on BD FACSVerse Flow Cytometer. Cells were collected and centrifuged at 300 x g for 5 minutes. The supernatant was aspirated. The cells were resuspended in flow buffer (PBS with %20 FBS) and the labeled-antibodies were added at recommended concentration. The cells were stained at room temperature for 20 minutes at dark. After incubation, the cells were pelleted and resuspended in PBS.

Discussion

In this study, we investigated the reasons for low transfection efficiency of unstimulated T cells. Unstimulated T cells are a mixture of naive, CM, EM, and EMRA cells. Although the frequencies of each subset differs from donor to donor, our analyses with multiple donors showed that naive cells were on average 50% of the whole population (Aksoy et al. 2018). Naive T cells are in the quiescent state and therefore are challenging to manipulate with a plasmid DNA. Because they are non-dividing cells, the nuclear envelope remains intact and the foreign plasmid DNA must be coupled to intracellular proteins to be imported into the cell nuclei (Bai et al. 2017). Accordingly, our imaging results showed more frequent nuclear localization of plasmids in activated cells compared to unstimulated cells.

To ameliorate the transfection efficiency of unstimulated cells, we tried to activate the cells immediately after electroporation. We hypothesized that when the cells commit to the cell cycle and proliferate due to activation signals, the plasmid DNA in the cytoplasm would be able to localize to the nucleus when the nuclear envelope disassembles. However, we did not observe a significant increase in transfection efficiency when we activated cells after electroporation. This might be due to the time it takes for unstimulated cells to start proliferating upon activation. It was suggested that the first cell division is completed around 30-48 hours post activation (Chapman and Chi 2018). It is possible that most of the plasmid DNA is degraded before the cell division occurs. Although we were able to detect labeled plasmid DNA one day after electroporation by fluorescence microscope, we should note that our labeling and detection methods were probably overestimating the frequency of plasmid positive cells 24h after electroporation considering that there was no way of discriminating between the fluorescence signals derived from intact or fragmented plasmid DNA.

Another reason why post activation upon electroporation did not work might be due to the differences in electroporation and transfection efficiencies of different subsets within the

unstimulated populations. Using a labeled plasmid, we showed that CM cells were the most electroporation- and transfection-efficient group within unstimulated pan T cells. However, these cells were the most vulnerable ones to plasmid DNA electroporation. Depletion and activation experiments showed that all of the naive enriched cells (CD45RO depletion group) that were activated became CMs and these had more proliferative capacity compared to the CMs within the unstimulated T cell population that was isolated from the PBMCs. Our results suggest an explanation for the well-known “donor effect” on transfection efficiencies for both unstimulated and activated cells: the more CM cells there are in a population, the better transfection efficiency is expected to be. Because CMs subset is the most proliferative subset among the others, it is not surprising that they are also the most transfection efficient ones. It was shown by 5-bromo-2’-deoxyuridine (BrdU) incorporation that actively dividing (BrdU positive) airway epithelia cells were 10 times more likely to express the transgene compared to BrdU negative ones (Fasbender et al. 1997).

Given that the nuclear localization of the plasmid DNA is one of the biggest challenges for transfection efficiencies of unstimulated T cells, manipulating the cells via *in-vitro*-transcribed mRNA or via Cas9 RNP should be relatively easy compared to plasmid DNA manipulation. An earlier study showed that unstimulated human T cells were electroporated with 95% transfection efficiency and 57% viability with an *in-vitro*-transcribed mRNA (Zhao et al. 2006). Similarly, a recent study suggested that efficient gene knock-out was possible for unstimulated T cells using Cas9 RNPs (Seki and Rutz 2018). Cas9 protein that is commercially available from various sources has the NLS tag fused to it, so trafficking of the Cas9 RNP complex into the nucleus is not a limiting factor in non-dividing cells. To increase the plasmid-based transfection efficiencies of unstimulated cells, plasmid DNA could be manipulated in a way that it harbors binding sites for cell-specific transcription factors or it could be complexed with a nuclear localization signals (NLS)-harboring protein prior to electroporation. Previous research has shown that coupling peptides harboring NLS to plasmid DNA either covalently or non-covalently can increase the transfection efficiency (Hébert 2003; Escriou et al. 2003). The success of non-covalent linkage was higher and this was probably due to transcriptional inhibition by the covalently linked NLS. One key study showed a significant improvement in transfection efficiencies in endothelium cells when the plasmid was complexed to a non-classical NLS harboring peptide: 5% transfection efficiency with plasmid alone and 83% with the NLS-peptide complex (Subramanian, Ranganathan, and Diamond 1999). These methods have yet to be implemented in T cell studies.

These improvements are of high importance to the field of cancer immunotherapy specifically for adoptive T cell transfer. For this type of therapy, manipulation of T cells is necessary to be able to directly target cancer cells. It has been described that early-lineage T cells do better in immunotherapy since they expand and persist more in the patients (Klebanoff et al. 2016; Busch et al. 2016). However, naive T cell manipulation is not a feasible option right now given the low transfection and transduction efficiencies of these cells. If the challenges that were outlined in this study can be overcome, then naive cells that are isolated from the patients’ blood can directly be manipulated before activation and expansion for reinfusion.

Acknowledgements

Supported in part by the Flow Cytometry and Cell Sorting Unit Shared Resource, Hollings Cancer Center, Medical University of South Carolina (P30 CA138313).

References

Aksoy, Bulent Arman, Pinar Aksoy, Megan Wyatt, Chrystal Paulos, and Jeff Hammerbacher. 2018. “Human Primary T Cells: A Practical Guide.” e26993v1. PeerJ Preprints. https://doi.org/10.7287/peerj.preprints.26993v1.

Bai, Haiqing, Gillian M. Schiralli Lester, Laura C. Petishnok, and David A. Dean. 2017. “Cytoplasmic Transport and Nuclear Import of Plasmid DNA.” *Bioscience Reports* 37 (6). https://doi.org/10.1042/BSR20160616.

Busch, Dirk H., Simon P. Fräßle, Daniel Sommermeyer, Veit R. Buchholz, and Stanley R. Riddell. 2016. “Role of Memory T Cell Subsets for Adoptive Immunotherapy.” *Seminars in Immunology* 28 (1): 28–34.

Czech, Eric, Bulent Arman Aksoy, Pinar Aksoy, and Jeffrey Hammerbacher. 2018. “Cytokit: A single-cell analysis toolkit for high dimensional fluorescent microscopy imaging” bioRxiv. 460980; doi: https://doi.org/10.1101/460980

Chapman, Nicole M., and Hongbo Chi. 2018. “Hallmarks of T-Cell Exit from Quiescence.” *Cancer Immunology Research* 6 (5): 502–8.

Escriou, Virginie, Marie Carrière, Daniel Scherman, and Pierre Wils. 2003. “NLS Bioconjugates for Targeting Therapeutic Genes to the Nucleus.” *Advanced Drug Delivery Reviews* 55 (2): 295–306.

Fasbender A, J Zabner, BG Zeiher & MJ Welsh. 1997. “A low rate of cell proliferation and reduced DNA uptake limit cationic lipid-mediated gene transfer to primary cultures of ciliated human airway epithelia.” *Gene Therapy* 4, 1173–1180.

Fraietta JA, Nobles CL, Sammons MA, Lundh S, Carty SA, Reich TJ et al. 2018. “Disruption of TET2 promotes the therapeutic efficacy of CD19-targeted T cells”. *Nature* Jun;558(7709):307-312.

Hébert, Eric. 2003. “Improvement of Exogenous DNA Nuclear Importation by Nuclear Localization Signal-Bearing Vectors: A Promising Way for Non-Viral Gene Therapy?” *Biology of the Cell / under the Auspices of the European Cell Biology Organization* 95 (2): 59–68.

Hinrichs, Christian S., Rosanne Spolski, Chrystal M. Paulos, Luca Gattinoni, Keith W. Kerstann, Douglas C. Palmer, Christopher A. Klebanoff, Steven A. Rosenberg, Warren J. Leonard, and Nicholas P. Restifo. 2008. “IL-2 and IL-21 Confer Opposing Differentiation Programs to CD8+ T Cells for Adoptive Immunotherapy.” *Blood* 111 (11): 5326–33.

Klebanoff, Christopher A., Luca Gattinoni, and Nicholas P. Restifo. 2012. “Sorting through Subsets: Which T-Cell Populations Mediate Highly Effective Adoptive Immunotherapy?” *Journal of Immunotherapy* 35 (9): 651–60.

Klebanoff, Christopher A., Christopher D. Scott, Anthony J. Leonardi, Tori N. Yamamoto, Anthony C. Cruz, Claudia Ouyang, Madhu Ramaswamy, et al. 2016. “Memory T Cell–driven Differentiation of Naive Cells Impairs Adoptive Immunotherapy.” *The Journal of*

Clinical Investigation 126 (1): 318–34.
Lea, Nicholas C., Stephen J. Orr, Kai Stoeber, Gareth H. Williams, Eric W-F Lam, Mohammad A. A. Ibrahim, Ghulam J. Mufti, and N. Shaun B. Thomas. 2003. “Commitment Point during G0-->G1 That Controls Entry into the Cell Cycle.” *Molecular and Cellular Biology* 23 (7): 2351–61.
McQuin C, Goodman A, Chernyshev V, Kamentsky L, Cimini BA, Karhohs KW et al. 2018. “CellProfiler 3.0: Next-generation image processing for biology”. *PLoS Biol.* https://doi.org/10.1371/journal.pbio.2005970
Reiser, John, and Arnob Banerjee. 2016. “Effector, Memory, and Dysfunctional CD8(+) T Cell Fates in the Antitumor Immune Response.” *Journal of Immunology Research* 2016 (May): 8941260.
Restifo, Nicholas P., Mark E. Dudley, and Steven A. Rosenberg. 2012. “Adoptive Immunotherapy for Cancer: Harnessing the T Cell Response.” *Nature Reviews. Immunology* 12 (4): 269–81.
Seki, Akiko, and Sascha Rutz. 2018. “Optimized RNP Transfection for Highly Efficient CRISPR/Cas9-Mediated Gene Knockout in Primary T Cells.” *The Journal of Experimental Medicine* 215 (3): 985–97.
Subramanian, A., P. Ranganathan, and S. L. Diamond. 1999. “Nuclear Targeting Peptide Scaffolds for Lipofection of Nondividing Mammalian Cells.” *Nature Biotechnology* 17 (9): 873–77.
Zhao, Yangbing, Zhili Zheng, Cyrille J. Cohen, Luca Gattinoni, Douglas C. Palmer, Nicholas P. Restifo, Steven A. Rosenberg, and Richard A. Morgan. 2006. “High-Efficiency Transfection of Primary Human and Mouse T Lymphocytes Using RNA Electroporation.” *Molecular Therapy: The Journal of the American Society of Gene Therapy* 13 (1): 151–59.

Supplemental Materials

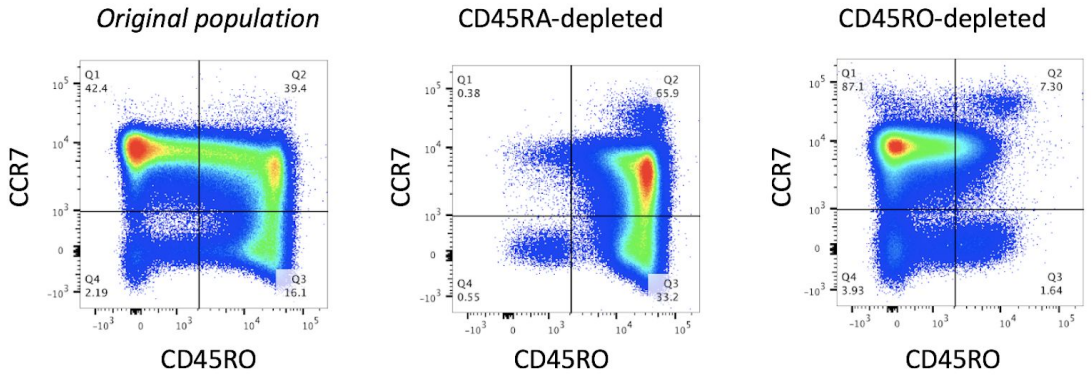

Supplemental Figure 1. Depletion of different groups by CD45RO and CD45RA antibodies and depletion Dynabeads. Following incubations with CD45RO and CD45RA antibodies, the cells were incubated with Dynabeads Pan Mouse IgG to deplete the antibody-bound population. This way, CD45RA incubation gave us the memory groups and CD45RO incubation gave us the naive and EMRA groups. The cells were stained with CCR7 (APC/Cy7) and CD45RO (APC) antibodies for analyzing them by flow cytometer to see the enrichment in subsets of cells.

Supplemental Table 1. Details of cellular characteristics inferred from fluorescence microscopy images of activated and unstimulated cells via Cytokit.

Experiment	20180911-D35-activated-labeled-60X-11by11	20180911-D35-unstimulated-labeled-60X-11by11	20180921-D34-act-lab-60X-15by15	20180921-D34-us-lab-60X-15by15	20181005-d37-act-lab-60x-19x19-take2	20181005-d37-unstim-lab-60x-19x19-take2	20181016-d38-act-lab-19by19-60x	20181016-d38-unstim-lab-19by19-60x
cells_per_sqmm_overall	1210.11	8709.36	627.975	4269.4	971.647	1233.35	171.665	1456.49
cells_per_sqmm_target	100.971	128.719	17.6165	135.129	17.826	9.68805	0.954452	4.36321
mean_cell_diameter	13.6997	8.25876	15.5385	8.59266	12.2213	8.37917	15.122	10.1386
mean_nucleus_diameter	8.02582	4.85701	9.01983	4.85302	7.20999	5.43356	9.25999	5.35117
mean_nucleus_to_cell_ratio	0.352117	0.367877	0.35295	0.335657	0.363202	0.439678	0.390034	0.299249
median_nucleus_to_cell_ratio	0.349692	0.357499	0.336009	0.321522	0.360909	0.441738	0.412458	0.292977
n_cells	262	334	85	652	138	75	7	32
pct_plasmid_in_nucleus	0.524109	0.180952	0.668675	0.166028	0.569231	0.358696	0.571429	0.081081
plasmid_count_dist	1 - 146 2 - 67 3 - 20 4 - 14 5 - 12 6 - 2 9 - 1	1 - 277 2 - 42 3 - 6 4 - 6 5 - 1 6 - 2	1 - 42 2 - 21 3 - 13 4 - 5 5 - 2 6 - 1 7 - 1	1 - 547 2 - 88 3 - 13 4 - 3 9 - 1	1 - 98 2 - 30 3 - 5 4 - 3 5 - 2	1 - 63 2 - 8 3 - 3 4 - 1	1 - 7	1 - 28 2 - 3 3 - 1